Intensive Working Memory Training Produces Functional Changes in Large-scale Frontoparietal Networks

Intensive Working Memory Training Produces Functional Changes in Large-scale Frontoparietal Networks

Todd W. Thompson[1,2]*, Michael L. Waskom[1,3]*, and John D. E. Gabrieli[1]

Abstract

■ Working memory is central to human cognition, and intensive cognitive training has been shown to expand working memory capacity in a given domain. It remains unknown, however, how the neural systems that support working memory are altered through intensive training to enable the expansion of working memory capacity. We used fMRI to measure plasticity in activations associated with complex working memory before and after 20 days of training. Healthy young adults were randomly assigned to train on either a dual *n*-back working memory task or a demanding visuospatial attention task. Training resulted in substantial and task-specific expansion of dual *n*-back abilities accompanied by changes in the relationship between working memory load and activation. Training differentially affected activations in two large-scale frontoparietal networks thought to underlie working memory: the executive control network and the dorsal attention network. Activations in both networks linearly scaled with working memory load before training, but training dissociated the role of the two networks and eliminated this relationship in the executive control network. Load-dependent functional connectivity both within and between these two networks increased following training, and the magnitudes of increased connectivity were positively correlated with improvements in task performance. These results provide insight into the adaptive neural systems that underlie large gains in working memory capacity through training. ■

INTRODUCTION

Effectively using working memory (WM) allows humans to maintain and manipulate goal-relevant information in the face of interference (Baddeley, 1992). WM capacity (WMC), the amount of information that an individual can hold in WM, is associated with performance on a wide range of cognitive tasks, including reasoning, problem solving, and reading comprehension (Engle, Tuholski, Laughlin, & Conway, 1999; Daneman & Carpenter, 1980), as well as academic performance (e.g., Finn et al., 2014; Gathercole, Pickering, Knight, & Stegmann, 2004). Although WMC has traditionally been conceptualized as a trait fixed before young adulthood, there is evidence that WMC can be increased in young adults who undergo adaptive WM training (reviewed in Klingberg, 2010). Furthermore, it has been suggested that gains in WM training might transfer to gains in broader reasoning abilities (Schweizer, Grahn, Hampshire, Mobbs, & Dalgleish, 2013; Jaeggi, Buschkuehl, Jonides, & Perrig, 2008). Although evidence for such "far transfer" after WM training is mixed (Redick et al., 2013; Thompson et al., 2013), participants consistently display impressive gains on the training task itself, typically doubling or tripling pretraining levels of performance (Kundu, Sutterer, Emrich, & Postle, 2013; Redick et al., 2013;

Thompson et al., 2013; Jaeggi et al., 2008). Furthermore, these gains are largely sustained over 6 months without further training (Thompson et al., 2013). Despite these observations, the functional brain plasticity that supports such large and enduring task-specific improvements following intensive long-term training remains poorly understood.

Although cognitive training has provoked substantial interest, previous fMRI studies of brain plasticity associated with WM training have been limited in two important ways: absence of an active control condition and a precise definition of which neural systems exhibit functional plasticity associated with expanded WM. Some studies have shown that short-term practice (Landau, Garavan, Schumacher, & D'Esposito, 2007; Kelly & Garavan, 2005; Landau, Schumacher, Garavan, Druzgal, & D'Esposito, 2004) or longer-term practice with a nonadaptive task (Hempel et al., 2004) can modify the relationship between WM demands and frontoparietal activation. Short-term nonadaptive training, however, does not produce large or enduring growth in WMC (Klingberg, 2010). Longer-term and adaptive WM training studies have reported disparate results after training. An early finding reported that increased WMC was associated with increased frontoparietal activation (Olesen, Westerberg, & Klingberg, 2004), whereas most subsequent training studies have observed decreased frontoparietal activation (Schweizer et al., 2013; Schneiders et al., 2012; Schneiders, Opitz, Krick, & Mecklinger, 2011).

[1]Massachusetts Institute of Technology, [2]Harvard Medical School, [3]Stanford University
*These authors contributed equally to this work.

Critically, none of these fMRI studies included an active control condition in which a control group performed an alternative adaptive cognitive training, so it is unknown whether previously reported training effects were specific to WM training or if the neural changes would have been seen with any intensive training task, regardless of cognitive domain. EEG studies with active control conditions have found electrophysiological changes in electrodes over frontoparietal regions after WM training, including increased network connectivity and increased power in theta bands during encoding (Kundu et al., 2013; Langer, von Bastian, Wirz, Oberauer, & Jäncke, 2013), but relative to fMRI, these EEG measures offer limited neuroanatomical specificity regarding the location of those changes.

Indeed, little is known about the mapping between the activation changes that accompany WMC expansion and the specific neural systems that support WM. Substantial neuroimaging evidence indicates that both dorsolateral pFC and posterior parietal cortex support WM through mechanisms of persistent activation (Curtis & D'Esposito, 2003; Cohen et al., 1997; Smith & Jonides, 1997). Activation in these regions parametrically scales with WM load or the amount of information that must be maintained (Braver et al., 1997; reviewed in Owen, McMillan, Laird, & Bullmore, 2005; Wager & Smith, 2003). Load-dependent activation further correlates with individual differences in WMC (McNab & Klingberg, 2008).

WM load-dependent effects on the brain are, however, spatially expansive and likely engage multiple component subsystems (Schweizer et al., 2013; Owen et al., 2005). In particular, frontoparietal association cortex contains two distinct large-scale networks associated with WM: the "executive control network" (ECN; identified as the "frontoparietal network" in Yeo et al., 2011, but renamed here for clarity), comprising dorsolateral and dorsomedial frontal nodes and a parietal node centered around the intraparietal sulcus, and the "dorsal attention network" (DAN), comprising the human FEFs and topographically mapped areas in the superior parietal lobe (Power et al., 2011; Yeo et al., 2011; Vincent, Kahn, Snyder, Raichle, & Buckner, 2008; Corbetta & Shulman, 2002). It is unknown as to whether training-related plasticity specifically occurs in one or both of these frontoparietal systems.

Here, we examined changes in neural function associated with large, enduring, and specific expansions of WMC in a randomized controlled trial. Two groups of young adults, matched for age, IQ, and gender, were randomly assigned to one of two adaptive training programs for 4 weeks (20 sessions). One group performed WM training on a dual n-back task (Jaeggi et al., 2008) and the other group (serving as an active control) performed a similarly intensive visuospatial training task involving multiple object tracking (MOT; Pylyshyn & Storm, 1988). A third group (serving as a passive control) performed the n-back task with the same pre–post interval, but without any training. Both training groups exhibited large and enduring task-specific gains that did not transfer be-

tween the two training tasks, whereas the passive group showed no improvement on either task (Thompson et al., 2013).

We examined the functional changes that were associated with the improvement in WM performance, measured both across the whole brain and specifically within the two major frontoparietal networks. Our analyses considered changes in both the magnitude of activation associated with WM as well as changes in functional connectivity within and between the two large-scale cortical networks. Finally, we assessed how the observed neural changes correlated with changes in task performance.

METHODS

Participants, Recruitment, and Group Assignment

Participants were recruited through web advertisements, physical flyers, and e-mail to the Northeastern University and Tufts University mailing lists. They were required to be adults between the ages of 18 and 45 years, right-handed, in good health, and not taking psychoactive medication. All participants provided informed written consent before participation. This study was approved by the Massachusetts Institute of Technology institutional review board (PI: Leigh Firn).

After recruitment, participants underwent pretraining behavioral testing to determine group assignment. Participants were initially sorted into one of two active training groups. Each participant was paired with another participant based on age, sex, and score on a preselected set of 18 of the 36 problems in the Raven's Advanced Progressive Matrices (RAPM; Raven, Court, & Raven, 1998), as described in Thompson et al. (2013). Each member of that pair was then randomly assigned to either the n-back or the MOT training group. MOT training was selected because the intensity and magnitude of task-specific learning were comparable to n-back training in a pilot study (Thompson, Gabrieli, & Alvarez, 2010), but gains in MOT performance did not transfer to other WM or executive function measures.

To control for performance improvements because of simple test–retest practice, we recruited a third matched passive control group that was examined twice with the same behavioral and neuroimaging measures and with the same interval between sessions as the training groups, but without any training. This group was recruited separately, but in the same fashion, and matched to a training pair by sex and initial RAPM score. Here, we use this passive control group to define independent ROIs for functional connectivity analyses, described below. The three groups did not differ significantly by gender [$\chi^2 (1, n = 37) = .21, p > .65$], RAPM scores [$t(1, 37) < 1, p > .48$], or on the full IQ score from the Wechsler Abbreviated Scale of Intelligence (Wechsler, 1999), administered as part of the pretraining battery [$t(1, 37) < 1,$

$p > .97$]. The passive control group averaged 1.8 years older than the two active training groups [$F(2, 55) = 3.37, p < .05$] (Table 1).

The training-based analyses reported here come from the 39 active training participants. Of those additionally recruited, 19 participants were assigned to the passive control group, and 14 potential participants either dropped out of the study or were excluded after initial scanning was completed. Two participants assigned to the dual n-back condition voluntarily withdrew (one after 5 days of training, the other after 9 days); no other participant had begun training when they were excluded or withdrew. The remaining potential participants were excluded for various logistical reasons, including difficulties aligning schedules with the experimenters, claustrophobia or excessive movement in fMRI scanning sessions, or repeatedly skipping pretraining appointments.

Participants were paid $20 per training session, with an additional weekly $20 bonus for completing all five training sessions in that week. Participants were paid $20 per hour for the initial and final behavioral testing sessions (approximately 3 hr each) and $30 per hour for neuroimaging sessions (2 hr pre- and posttraining of fMRI, 1 hr of electroencephalography). Total compensation for each participant completing the experiment was approximately $900.

Overall Experiment Design

After recruitment, participants completed baseline behavioral testing (described in Thompson et al., 2013) and a pretraining imaging session that included structural scans for anatomical registration and four runs of the dual n-back task described below. They then completed 20 sessions of adaptive training on either the n-back or MOT task while at the Massachusetts Institute of Technology campus. In the dual n-back task, successful performance increased the "n" in the n-back, whereas successful performance in the MOT training task increased the speed of the tracked objects but did not affect the number of objects to be tracked. After training was completed, behavioral testing and posttraining imaging were administered as quickly as possible. The average number of days between the last training session and posttraining testing was 4.3 days, with a minimum of 0 days and maximum of

14 days. This time was not significantly different between the two training groups [$t(37) = 0.2, p > .8$]).

Dual n-back Functional Imaging Task Description

Implementation of the adaptive dual n-back training task followed Jaeggi et al. (2008). An auditory letter and a visual square were simultaneously presented for 500 msec, followed by a 2500-msec response period. Letters were chosen from the consonants B, F, H, J, M, Q, R, and W to maximize auditory discriminability between letters. Squares were presented at one of eight positions evenly spaced around the periphery of the screen. Participants responded when one or both of the current stimuli matched a stimulus presented n trials ago. In the "0-back" condition, participants were instructed to respond to a spatial target in the top right corner as a visual match or to the letter "Q" as an auditory match. To ensure that each participant fully understood the task, at least one block of each difficulty level was practiced outside the scanner, and participants were allowed to repeat this practice task as necessary until they reported full understanding of the instructions. In addition to the task practice before both of the pre- and postscanning sessions, participants had completed a behavioral dual n-back testing session in the days prior to each scan, which lasted approximately an hour, and measured baseline performance on dual n-back loads of 1–6. This process familiarized participants with the task before scanning and ensured that the MOT group remained familiar with the task after the training period.

Each block in the imaging version of the task presented 10 trials, containing two auditory targets and two visual targets, with no trials where both auditory and visual stimuli matched. To ensure a consistent level of difficulty between blocks of a given load, trials that would have matched either the $n + 1$ or $n - 1$ stimulus ("lure trials") were not included. During each block, the current load was indicated at a central fixation point along with additional text labels showing the mapping between the two response buttons and "Audio" or "Video" match types.

Responses were made using a scanner-compatible button box that the participant held in the right hand. A press of the first button, under the participant's index

Table 1. Participant Demographics

Group	Total n (No. of Women)	Age,[a] yr	IQ[a]	RAPM[a]
MOT	19 (11)	21.3 (2.3)	120.7 (7.0)	13.8 (2.3)
n-back	20 (13)	21.2 (2.0)	120.9 (10.8)	13.4 (2.1)
Passive control	19 (12)	23.1 (3.3)	117.6 (7.4)	13.3 (2.2)

IQ measure is the Full 4 IQ measure from the Wechsler Abbreviated Scale of Intelligence. RAPM measure reflects the number of problems solved on half of the RAPM (see Thompson et al., 2013, for RAPM details).

[a]Standard deviation in brackets.

finger, indicated auditory matches, and a press of the second button, under the middle finger, indicated spatial matches. No response was required on trials that did not match the target. Participants were allowed the entire 3 sec following the onset of stimulus presentation to make a response.

Each dual *n*-back run consisted of eight 30-sec blocks of the dual *n*-back task, with two blocks of each load from 0-back to 3-back. The order of the blocks was counterbalanced across the four total runs. Each block was preceded by a 3-sec instruction screen indicating the *n*-back load for the upcoming block and was followed by 16 sec of rest to let the hemodynamic response return to baseline. The total acquisition time for each run was 6 min and 36 sec. Each participant completed four runs of the dual *n*-back task before and after training. In summary, there were 10 trials per block and eight blocks for each load, equating to 80 total stimulus presentations at each load. In four cases, scanning delays prevented acquisition of the last run. This occurred once in a pretraining *n*-back participant, twice in pretraining MOT participants, and once in a posttraining MOT participant.

MRI Data Acquisition

Whole-brain imaging was performed on a 3T Siemens Tim Trio MRI system using a 32-channel head coil. Functional images were obtained using a standard T2*-weighted echo-planar pulse sequence (repetition time = 2 sec, echo time = 30 msec, flip angle = 90°, 32 slices, 3.0 × 3.0 × 3.1 mm voxels, 20% slice gap, axial interleaved acquisition). Prospective adaptive motion correction was employed to minimize the effects of participant motion. For steady state magnetization, 8 sec of dummy scans were collected at the beginning of each run, before the experimental paradigm began. Additionally, a whole-brain high-resolution T1-weighted multiecho MP-RAGE anatomical volume was acquired for purposes of cortical surface modeling, registration to common anatomical space, and across-run alignment (repetition time = 2.5 sec, echo time = 1.64, 3.5, 5.36, and 7.22 msec, 176 slices, 2× GRAPPA acceleration, field of view = 256 mm). Visual stimuli were projected onto a screen at the back of the scanner and viewed through a mirror attached to the head coil.

Data Analysis

In-scanner dual n-*back performance.* To control for response biases between participants, performance was characterized as hit rate − false alarm rate within each level from 0-back to 3-back. Repeated-measures ANOVAs were evaluated on this dependent variable with Training group as a between-subject factor and Task load and Session (pre- or posttraining) as within-subject factors.

Functional imaging analysis procedure. Functional imaging data were processed with a workflow of FSL (Smith et al., 2004) and Freesurfer tools (Dale, Fischl, & Sereno, 1999) implemented in Nipype (Gorgolewski et al., 2011). Each time series was first realigned to its middle volume using normalized correlation optimization and cubic spline interpolation. Next, a mask of brain voxels was estimated to constrain later procedures. Images with artifacts were automatically identified as those frames on which total displacement relative to the previous frame exceeded 1 mm or where the average intensity within the brain mask deviated from the run mean by greater than three standard deviations. The functional data were spatially smoothed with a 6-mm FWHM kernel using the SUSAN algorithm from FSL, which restricts smoothing to voxels of similar intensity (Smith & Brady, 1997). Finally, the time series data were high-pass filtered by fitting and removing Gaussian-weighted running lines with an effective cycle cutoff of 160 sec.

Separately, the T1-weighted anatomical volume was processed using Freesurfer to segment the gray–white matter boundary and construct tessellated meshes representing the cortical surface (Dale et al., 1999). Functional data from each run were then registered to the anatomical volume with a six-degree-of-freedom rigid alignment optimizing a boundary-based cost function (Greve & Fischl, 2009). The anatomical image was separately normalized to MNI152 space using FSL's nonlinear registration algorithm (Jenkinson, Beckmann, Behrens, Woolrich, & Smith, 2012). Following these steps, the linear functional-to-anatomical transformation matrix was combined with the nonlinear anatomical normalization parameters to derive a single transformation from native run space to MNI152 space.

Parametric load analysis. A linear model was fit separately to each functional time series using Gaussian least squares with local correction for temporal autocorrelation (Woolrich, Ripley, Brady, & Smith, 2001). A single task regressor with boxcar functions indicated the task load, with 0-back, 1-back, 2-back, and 3-back blocks modeled with a −3, −1, 1, and 3 weights, respectively. A separate column of 1 sec modeled the main effect of Task. Additionally, the instruction period before each block was modeled with a separate regressor. These regressors were then convolved with the canonical difference-of-gammas hemodynamic response function from the FSL software package (Jenkinson et al., 2012). In addition to the artifact indicator vectors described above, we included regressors for the six realignment parameters used during motion correction (i.e., translations along and rotations around the three main axes in native participant space) to account for residual noise variance introduced by participant motion. Following model fitting, the contrast effect size and standard error images were normalized to group space using the transformation described above and resampled with trilinear interpolation. Contrast effects were then combined across runs using a subject-level fixed effects model.

Mixed-effects higher-level analyses were used to model the parametric effect of load within the MOT and dual *n*-back groups independently for the pre- and posttraining scans. The resulting contrast estimates were then entered into a higher-level random effects model to determine both the longitudinal effect of training within each group and the Group by Time interaction. Correction for multiple comparisons was accomplished by first thresholding resulting whole-brain maps at a *z*-score of 2.3 and then cluster-correcting to control the family-wise error rate at $p < .05$.

Analysis of independent load contrasts. This model was identical to the parametric model described above but replaced the single parametric task regressor with four independent regressors, one for each of the *n*-back difficulty levels, with boxcar functions indicating the task blocks.

Regions/networks of interest analysis. In addition to the whole-brain univariate approach, we also performed focused analyses within the ECN and DAN ROIs derived from a population atlas of task-independent cortical networks (Yeo et al., 2011). As this atlas is defined in Freesurfer's common surface space, region labels were first warped back to the individual participant surfaces by inverting the spherical normalization parameters obtained during cortical reconstruction. Vertex coordinates within each of these labels were then transformed into the native functional space by inverting the linear functional-to-anatomical transformation for the first run. Finally, voxels were identified for inclusion within each region's ROI mask by projecting half the distance of the cortical thickness at each vertex and labeling the intersected voxels. This method produced ROIs that reflected the underlying two-dimensional topology of the cortex and minimized the inclusion of voxels lying outside gray matter.

Performance-weighted load analysis. We further explored how BOLD activation within the ECN and DAN related to WM load using a performance-weighted analysis. In this analysis, we regressed mean BOLD activation at each *n*-back level against a weighted *n*-back variable formed by multiplying the "*n*" of the current level by each participant's behavioral performance (hit rate − false alarm rate) at that level, thus scaling "*n*" to an estimate of the actual WM load. As in the parametric analysis described above, the resulting regression coefficient describes the relationship between WM load and BOLD activation. To test whether training influenced this relationship and whether that influence differed in the two large-scale networks, we applied linear mixed effects models using the R package nlme (Pinheiro, Bates, DebRoy, Sarkar, & R Core Team, 2015).

Functional connectivity analysis. Functional connectivity within task-activated (task-positive) regions was assessed using seed-based time series correlations. Connectivity analyses can be particularly sensitive to misspecification of nodes (Smith et al., 2011) so we constrained analyses to regions that were reliably active before training. We used data from the passive control group's first scanning session, which allowed us to define regions that were statistically independent from the main analysis and to avoid the concern that the selected ROIs might be biased toward one training group's pretraining activations. Because the greatest training-related activation changes occurred in the 2-back condition (reported below), the passive control group's 2-back versus baseline contrast was used to obtain functional connectivity seeds. The positive activations from this contrast were thresholded at $p < .001$, then cluster-corrected at $p < .05$. The resulting clusters were then intersected with an anatomical mask from the Harvard–Oxford atlas that included lateral prefrontal and parietal cortex. This approach yielded four ROIs: one prefrontal ROI and one parietal ROI in both the right and the left hemisphere. Each ROI was then reverse-normalized into native space using the surface-based approach described above and intersected with the subject-specific DAN and ECN masks, thus yielding 12 ROIs in total per participant (four whole cluster ROIs, four DAN ROIs, and four ECN ROIs).

For each prefrontal ROI in each participant, the experimental time course was extracted using the mean activity of all voxels within the ROI at each time point. For a given *n*-back level, the portions of the time course corresponding to seconds 8–30 of each *n*-back block were preserved (the first 3 volumes were omitted to avoid artifactual correlations emerging from the rising hemodynamic response), whereas the remainder of the time course was set to 0.

A general linear model was then created for each ROI using its specific *n*-back time course as the regressor of interest and including traditional block regressors for the other three conditions, along with the artifact indicator vectors and motion parameter nuisance regressors described above. Finally, six additional nuisance regressors were included representing the first six principal components of the white matter and CSF time course, which were extracted using the subject-specific Freesurfer mask of white matter and CSF. Before extraction, this mask was eroded by two voxels to avoid contamination from partial voluming with gray matter voxels.

These models were then processed as described above through the fixed effects analysis for each subject, using FSL. Finally, for each of the prefrontal ROI models, the mean parameter estimate was extracted to measure functional connectivity between that prefrontal ROI and each of the parietal ROIs. Higher-level analyses were performed on these parameter estimates using a Group × Session mixed-effects ANOVA separately for the 1-back, 2-back, and 3-back levels. We specifically examined connectivity between the whole-cluster ROIs and, separately, connectivity both within and between the DAN and ECN

ROIs. Analyses were corrected for multiple comparisons using Bonferroni adjustments across pairs of ROIs and, where applicable, n-back levels.

Connectivity/behavioral correlations. After observing training-related changes in network connectivity, we assessed the relationship between those changes and training-related changes in performance on the in-scanner dual n-back task by calculating the Pearson correlation between the change in functional connectivity and the change in behavioral performance across participants.

RESULTS

Behavioral Results

Baseline Performance

Before training, increasing dual n-back loads resulted in significantly decreasing accuracy (measured as hit rate − false alarm rate) [one-way ANOVA $F(3, 114) = 108.3, p < .001$] and increasing RT [$F(3, 114) = 125.1, p < .001$] (Figure 1). There were no significant baseline differences between the two training groups on either accuracy ($ps > .11$) or RT ($ps > .14$).

Changes in Performance after Training

Four weeks of adaptive dual n-back training selectively improved performance on the dual n-back task in the
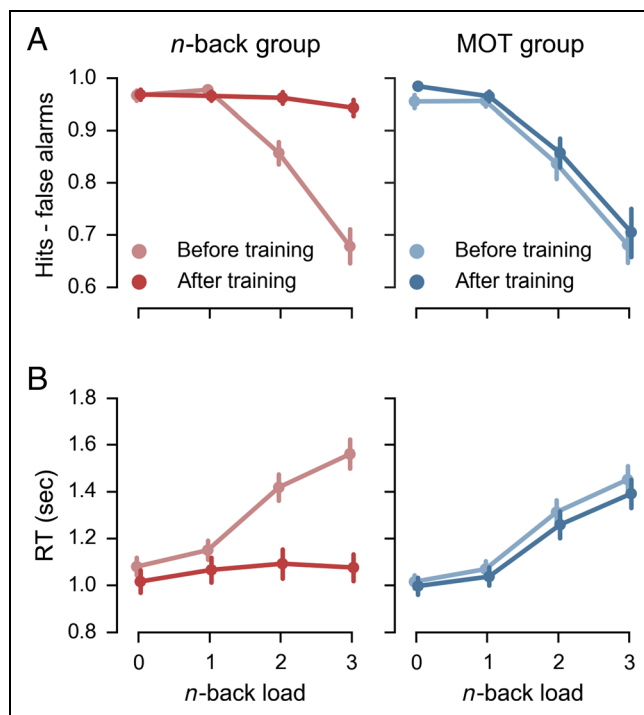

Figure 1. Adaptive dual n-back training selectively facilitates performance on the n-back task. (A) Corrected hit rates for in-scanner n-back performance for each training group. (B) In-scanner reaction times for each training group. Error bars represent *SEM*.

scanner (Figure 1A). A mixed-design ANOVA examining Session × n-back load × Group for accuracy revealed that there were significant main effects of Load [$F(3, 137) = 85.9, p < .001$], Session [$F(1, 37) = 30.9, p < .001$], and Group [$F(1, 37) = 5.84, p = .021$], and significant interactions of Group × Load [$F(3, 111) = 6.22, p < .001$], Group × Session [$F(1, 37) = 11.8, p = .002$], Load × Session [$F(3, 111) = 24.4, p < .001$], and Group × Load × Session [$F(3, 111) = 21.3, p < .0001$]. Thus, performance decreased as load increased, improved after training, and was better in the n-back group than in the MOT group. Critically, the improvements across sessions were specific to n-back training. In mixed Session × Load analyses within each training group, the n-back group performed significantly better after training [main effect of session $F(1, 19) = 32.8, p < .001$], whereas the MOT group did not improve significantly after training [main effect of Session $F(1, 18) = 2.7, p > .11$].

To better understand the results from the omnibus ANOVA, Session × Group ANOVAs were performed separately for each load. Mixed-design ANOVAs showed that the omnibus interaction was driven by significant Group × Session interactions only at the dual 2- and 3-back loads in which the n-back group became more accurate after training than did the MOT training group [0-back $F(1, 37) = 2.2, p = .14$; 1-back $F(1, 37) = 1.6, p = .21$; 2-back $F(1, 37) = 5.8, p = .02$; 3-back $F(1, 37) = 28.7, p < .001$].

Analyses of RTs revealed a similar pattern to that seen with accuracies. After training, the n-back group responded significantly faster than they had before training (Figure 1B) and improved their response times more than did the MOT group. A mixed-design ANOVA examining Session × Load × Group showed significant main effects of Load [$F(3, 137) = 101.8, p < .001$] and Session [$F(1, 37) = 44.3, p < .001$] but no main effect of Group [$F(1, 37) = 0.02, p = .88$]. However, there were significant interactions of Group × Load [$F(3, 111) = 5.33, p = .002$], Group × Session [$F(1, 37) = 21.3, p < .001$], Load × Session [$F(3, 111) = 30.7, p < .001$], and Group × Load × Session [$F(3, 111) = 20.4, p < .0001$]. In mixed Session × Load analyses within each training group, both the n-back group [main effect of Session $F(1, 19) = 39.0, p < .001$] and the MOT group [main effect of Session $F(1, 18) = 5.5, p = .03$] responded significantly faster after training, although the gain in speed was significantly greater in the n-back group than the MOT group as reflected in the Group × Session interaction.

The omnibus interaction was most influenced by faster RTs in the n-back group after training at the more difficult loads. Specifically, mixed-effects Group × Session ANOVAs run at each n-back load independently showed that the Group × Session × Load interaction was driven by changes in RT at the dual 2-back and 3-back loads [0-back $F(1, 37) = 1.1, p = .30$; 1-back $F(1, 37) = 1.15, p = .29$; 2-back $F(1, 37) = 16.7, p < .001$; 3-back $F(1, 37) = 48.8, p < .001$].
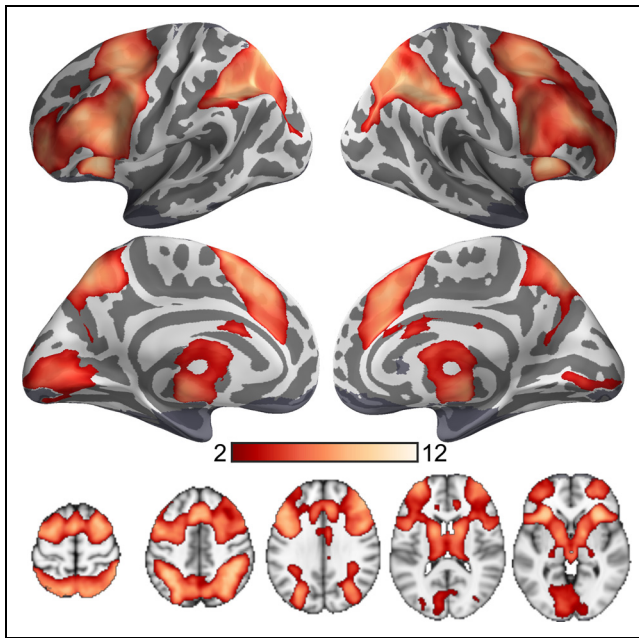
Figure 2. Brain regions exhibiting significant increases in activation as a function of WM load in all participants (*n* = 39). Statistical inferences derived from volume-based analysis but projected onto Freesurfer average cortical surface mesh for visualization.
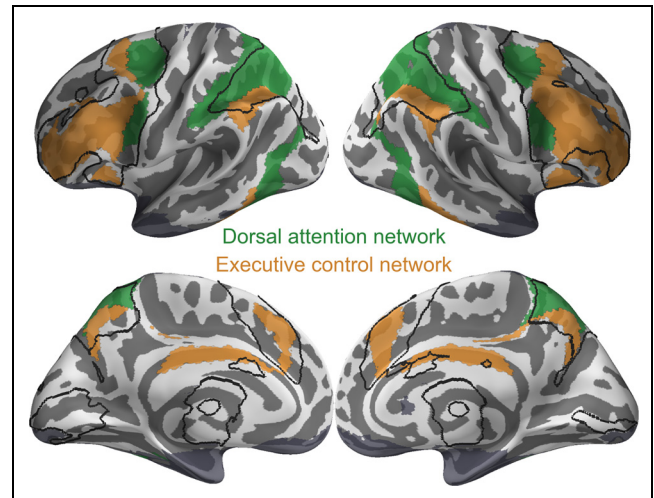

Figure 3. Baseline load-dependent WM activation occurs in ECN and DAN. ECN (orange) and DAN (green) defined anatomically and independently from resting-state networks (Yeo et al., 2011). Regions of load-dependent activation are outlined in black and substantially overlap ECN and DAN networks bilaterally.

occurred bilaterally in both the ECN and DAN (Figure 3) as characterized by a group atlas of resting-state networks (Yeo et al., 2011).

Univariate Imaging Results

Training-related Changes in Load-dependent Activation

Regions exhibiting training-dependent changes in activation were identified in a repeated-measures model using the Session × Group interaction. The *n*-back group

Load-dependent Activations before Training

Across both training groups, activations increased as a function of WM load in many regions, including lateral and medial prefrontal regions, parietal regions, anterior insula, and subcortical regions in the BG and thalamus (Figure 2 and Table 2). These load-dependent activations

Table 2. Regions Parametrically Activated by Dual *n*-back Load

Cluster	Peak Z-value	X	Y	Z	Region
Anterior	9.76	32	22	2	Insular cortex
	9.59	−32	24	2	Insular cortex
	8.81	30	10	60	Middle frontal gyrus
	8.78	0	14	54	Superior frontal gyrus
	8.69	−46	24	30	Middle frontal gyrus
	8.61	44	34	28	Middle frontal gyrus
Posterior	10.00	44	−42	48	Posterior supramarginal gyrus
	9.76	−38	−48	42	Posterior supramarginal gyrus
	8.53	−10	−68	60	Superior lateral occipital cortex
	8.16	32	−70	52	Superior lateral occipital cortex
	3.28	20	−56	24	Precuneus cortex
	2.42	−30	−84	6	Inferior lateral occipital cortex

Local maxima for the linear effect of WM load, collapsing across training groups at the pretraining scan (*n* = 39). Statistical thresholding identified two major clusters of activation; local maxima are reported for peaks within these clusters separated by a minimum distance of 30 mm. Coordinates are reported in the FSL MNI152 space.
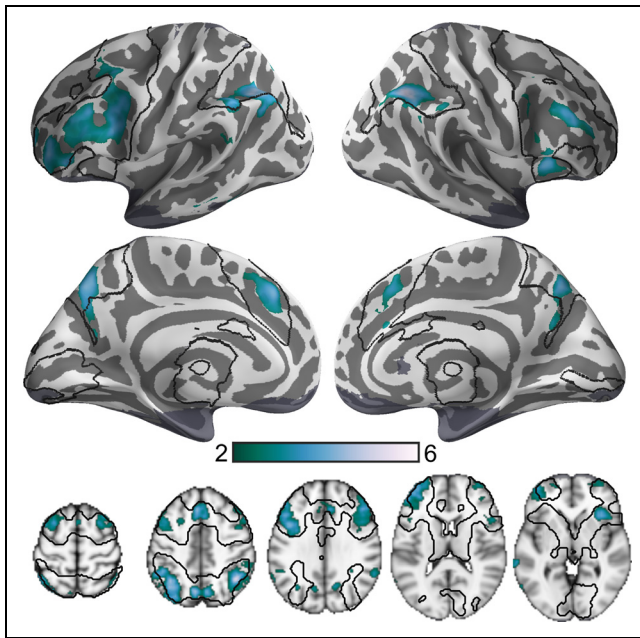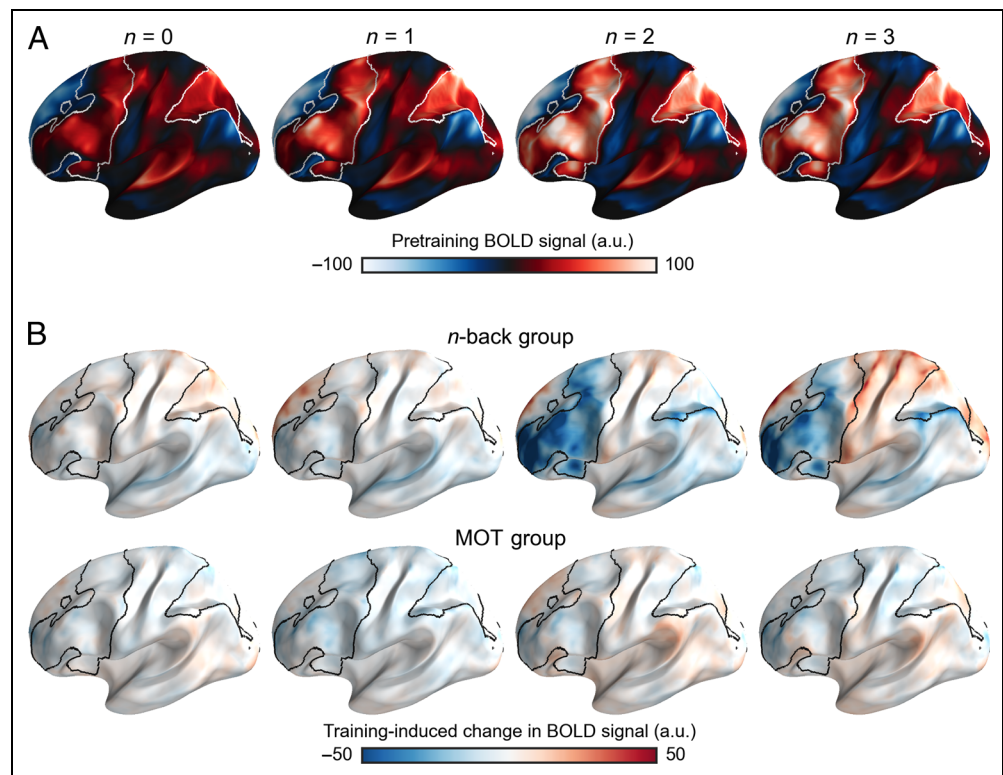
Figure 4. Dual *n*-back training reduces load-dependent activation. Results are shown for a Group × Time interaction analysis on the parametric effect of WM load. Black outlines indicate the extent of load-modulated regions in the pretraining analysis (Figure 2). Image presentation is otherwise identical to Figure 2.

3-back loads and were most pronounced for the 2-back load (Figure 5).

Relation of Training-related Reductions of Activation to ECN and DAN

ROI analyses confirmed that the *n*-back group exhibited a greater reduction of the relationship between WM load and activation in the ECN than in the DAN (Figure 6). We extracted activation coefficients for each *n*-back load from the independently defined ECN and DAN (Yeo et al., 2011). A mixed-effect ANOVA on these values revealed a significant four-way Load × Network × Session × Group interaction [$F(3, 111) = 9.14, p = .003$]. Before training, activation in both networks increased as a function of WM load. Dual *n*-back training-induced activation changes in the ECN were significantly greater than those in the DAN as measured by a Load × Network × Session interaction [$F(3, 57) = 25.9, p < .001$], with the ECN displaying substantially reduced activations at the 2-back and 3-back loads. Consistent with the prior analyses, there was no significant change in activation in either network for the MOT training group.

Performance-weighted Analyses of the Relationship with WM Load

An alternate approach to identifying regions responsible for task performance directly includes participant performance in the model. These results are largely consistent

exhibited significantly reduced load-dependent responses after training in prefrontal, parietal, and insular cortical regions (Figure 4). Training-induced changes in BOLD activation were primarily observed at 2-back and

Figure 5. Only the *n*-back group exhibited reductions of activation after training in the 2-back and 3-back conditions. (A) Mean BOLD signal, relative to baseline. (B) The mean difference between pre- and posttraining BOLD signal (changes from implicit baseline) is shown for each *n*-back level for *n*-back group (top row) and MOT group (bottom row). In both panels, the outlines correspond to the extent of activations identified using a parametric analysis as shown in Figure 3.

Figure 6. *n*-back training dissociates the contribution of ECN and DAN to WM. Mean activation coefficients for each *n*-back load relative to rest blocks were extracted from the ECN and DAN and plotted separately for each session and training group. Error bars represent *SEM*.
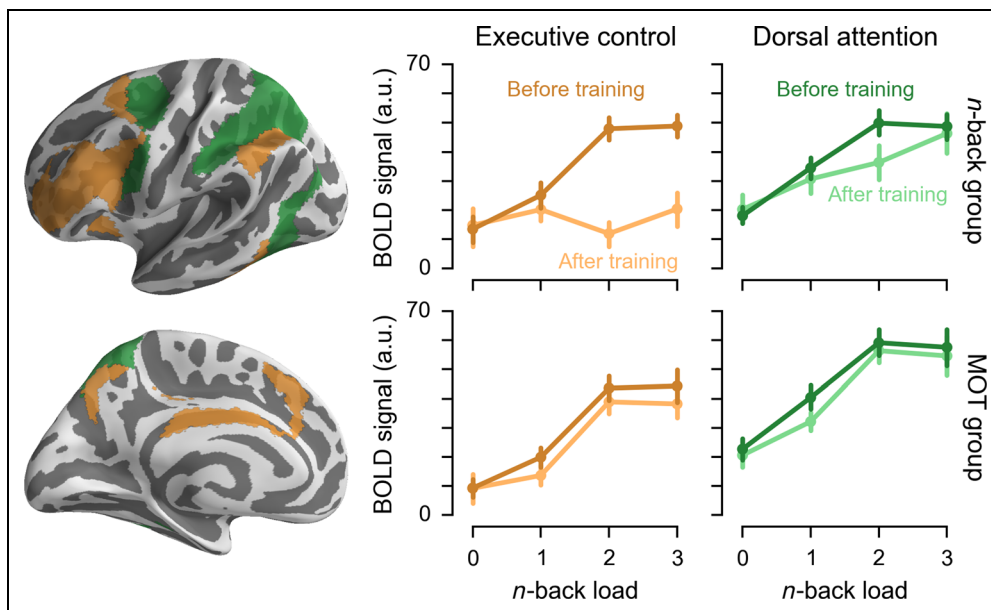
with the previous load-dependent analysis but reveal additional nuances of the training-related changes (Figure 7). BOLD responses in both the E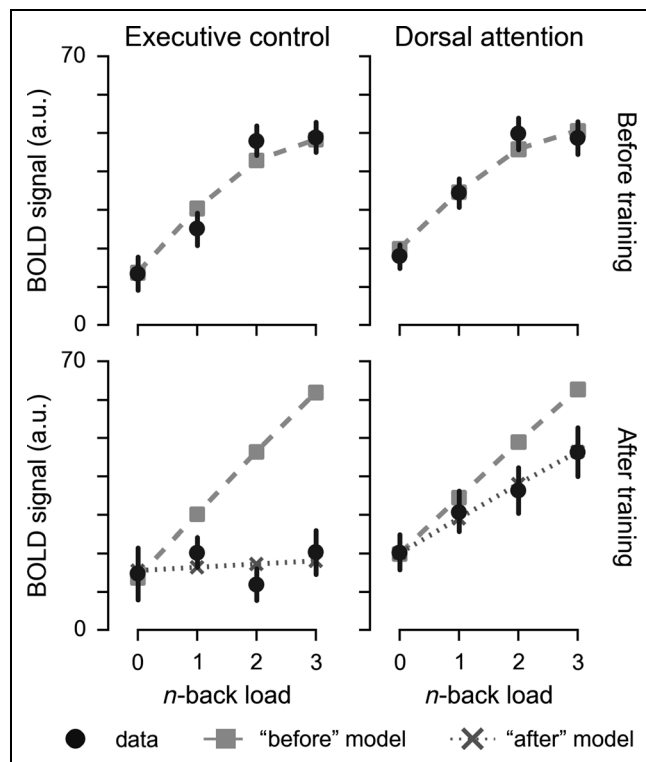CN [$F(1, 59) = 101.5, p < .001$] and DAN [$F(1, 59) = 70.7, p < .001$] were significantly and positively related to participant performance at a given load before training. In both the ECN and DAN, training reduced the relationship between activation and load [ECN Load × Session interaction $F(1, 137) = 41.8, p < .001$; DAN Load × Session interaction $F(1, 137) = 13.3, p < .001$], but the reduction of that relationship was significantly greater in the ECN [Load × Session × Network interaction $F(1, 239) = 9.7, p = .002$]. DAN activation, unlike ECN activation, remained significantly related to WM load in the posttraining session [main effect of Load in DAN $F(1, 59) = 24.2, p < .001$; main effect of Load for ECN $F(1, 59) = .16, p > .68$].

Figure 7. Performance-weighted analysis of relationship between WM load and BOLD activation. Black circles show mean BOLD signal, along with standard errors, as in Figure 6. Gray squares show the predictions of a performance-weighted model fit to the BOLD data from before training. Gray Xs show the predictions of a performance-weighted model fit to the BOLD data after training. Results are shown only for the *n*-back training group.

Frontoparietal Functional Connectivity

Changes with Training

We examined training-related changes in functional connectivity (BOLD time series correlations) during task performance between left and right prefrontal and parietal ROIs defined using pretraining activations in the passive control group. For each pair of ROIs in the dual 1-, 2-, and 3-back conditions, a Session × Group interaction measure was calculated from a mixed-effects ANOVA. Significant *n*-back training-induced increases in functional connectivity were observed for all four pairings of prefrontal and parietal ROIs in the 2-back condition ($p < .05$, Bonferroni-corrected across load and connection), but no changes were observed in the 1- or 3-back conditions (Figure 8A). We then divided each ROI into ECN and DAN components using the Yeo network ROIs. In contrast to the asymmetric findings of the univariate analysis, in which the ECN exhibited substantively larger changes than did the DAN, this analysis revealed significantly increased connectivity between nodes of the ECN, between nodes of the DAN, and also for between-network

Figure 8. Training increased frontoparietal functional connectivity in *n*-back group. (A) Group by session interaction measures, showing group differences in the change of functional connectivity strength. Positive values indicate greater connectivity after training for the *n*-back group relative to the MOT group. Each bar shows the change in connectivity for a pair of frontal and parietal ROIs (collapsed across ECN and DAN networks). (B) Group by session interaction measures during 2-back blocks for ROIs defined using functional activations within and between resting-state networks. Error bars in (A) and (B) represent *SEM*. (C) Change in functional connectivity strength for each pair of ROIs, as shown in (B). The weight of the edge indicates the Bonferroni-corrected *p* value for the group by session interaction. (D) Scatterplot showing the relationship between the change in behavioral performance and the change in functional connectivity in 2-back blocks. The functional connectivity measure is averaged across the four edges shown in (A). (E) Scatterplot showing the correlation of each node-to-node connectivity change with the change in behavioral performance.
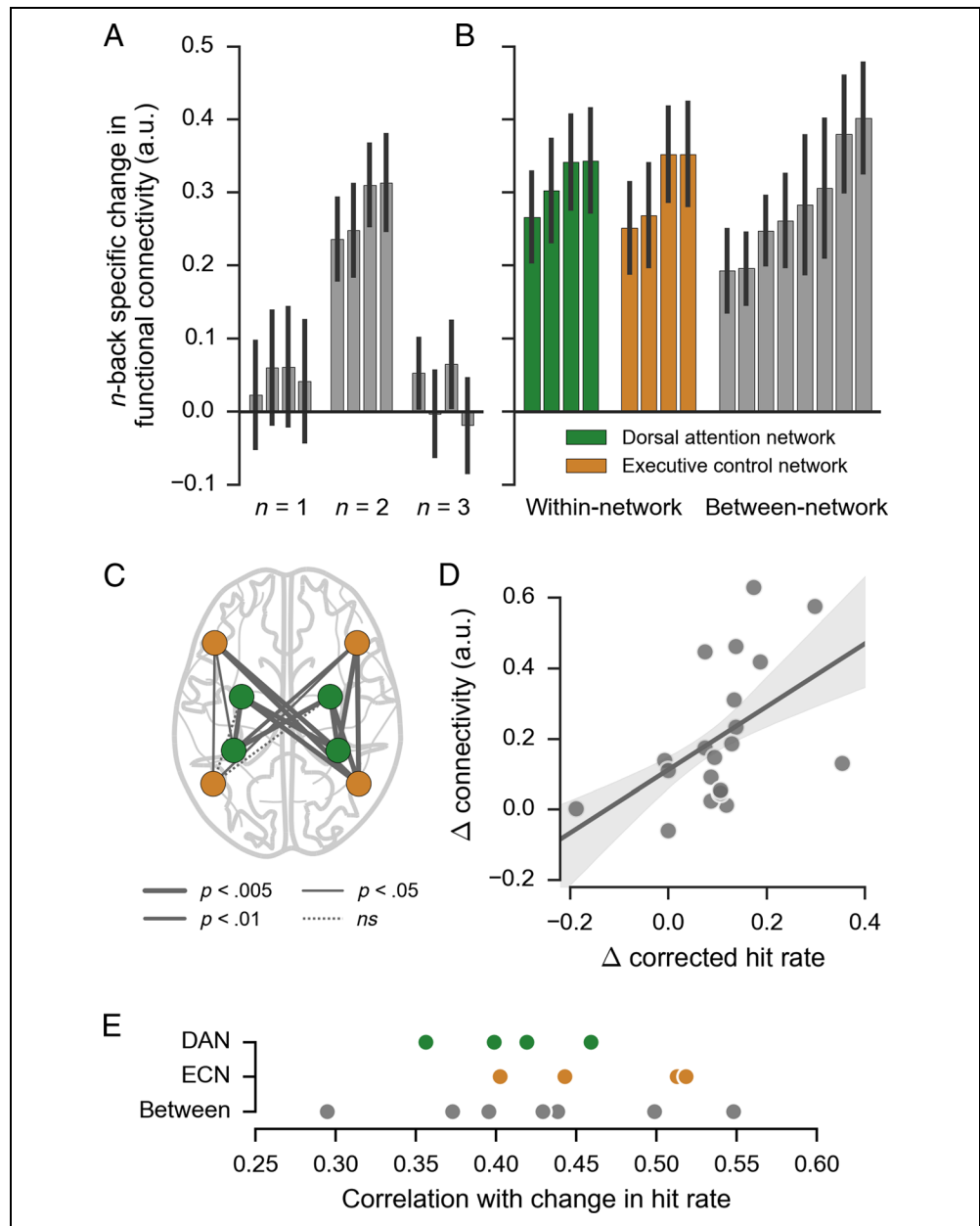
connections ($p < .05$, Bonferroni-corrected across connection; Figure 8B, C).

Correlations between Connectivity Changes and In-scanner Performance

Pre–post training accuracy improvements among participants in the *n*-back group in the dual 2-back scanner task were positively correlated with their increases in functional connectivity within the four frontoparietal pairings displayed in Figure 8A ($r = .50$, $p = .03$; Figure 8D). These correlations were not driven by any specific node to node (Figure 8E). Connectivity increases were not significantly correlated with changes in RTs ($r = .20$, $p > $

.39). There were no significant correlations between accuracy improvements and univariate activation changes.

DISCUSSION

Functional brain plasticity associated with a large increase in dual *n*-back performance was characterized as highly specific in multiple ways. First, learning occurred selectively in the *n*-back training group, who displayed marked gains on the trained task (Thompson et al., 2013), and not in the MOT training group, who showed neither behavioral improvements nor brain plasticity associated with the dual *n*-back task. This is the first fMRI evidence that such plasticity is specific to WM training

and not a consequence of any intensive and adaptive training program. Second, the *n*-back training group showed both behavioral gains and reduced activation selectively for the WM-demanding 2-back and 3-back conditions. Third, although both the ECN and DAN fronto-parietal networks demonstrated load-dependent activation before training, training produced a dissociation between these networks and eliminated the relationship with WM load selectively within the ECN. Fourth, the ECN and DAN both exhibited training-selective increases in functional connectivity, which were correlated with corresponding improvements in behavioral performance. This finding indicates that brain plasticity resulting from intensive WM training occurs not only in terms of activation magnitudes, but also in relation to altered network functional connectivity.

Pretraining Activation in Dual *n*-back Task

The pattern of load-dependent activation at pretraining was generally consistent with prior neuroimaging studies, which have typically reported activations in dorsolateral and ventrolateral pFC, frontal poles, lateral and medial premotor cortex, dorsal cingulate, and medial and lateral posterior parietal cortex (Owen et al., 2005). Specific patterns of activation have varied in relation to stimulus and task dimensions, and only three fMRI studies have examined the functional activations associated with a simultaneous visual–spatial and auditory–verbal dual-back task (Buschkuehl, Hernandez-Garcia, Jaeggi, Bernard, & Jonides, 2014; Jaeggi et al., 2007; Yoo, Paralkar, & Panych, 2004). The pattern of load-dependent activation observed here, including frontal, parietal, temporal, and subcortical activations, resembles those reported in the prior dual *n*-back studies.

Training-related Activations in Dual *n*-back Task

Functional brain changes mirrored behavioral changes in performance after training. The MOT group exhibited no improvement in dual *n*-back capacity despite great improvement on the MOT task (Thompson et al., 2013) and also exhibited no difference across sessions in functional activation. The *n*-back group showed no gain in performance for the 0-back and 1-back conditions, presumably performing at ceiling from the outset, and exhibited no difference across sessions in functional activation at those loads. The training did, however, substantially improve performance in the more demanding 2-back and 3-back conditions, which the *n*-back group performed with the same ease (measured by accuracy and RT) as the 0-back and 1-back conditions after training. Correspondingly, there were significant and widespread reductions in activation, most notably in bilateral inferior and middle frontal gyri, insular cortex, and intraparietal sulci.

Frontal and parietal regions were divided into two independent systems, the ECN and the DAN, based on a group atlas of resting-state networks (Yeo et al., 2011). Activation in both networks exhibited a strong relationship with WM load in the initial session, but training produced a dissociation between the two networks. After training, activation in the DAN remained significantly related to WM load but was no longer related to WM load in the ECN. This dissociation provides a novel perspective on the distinct roles of those frontoparietal systems. Although both networks are thought to play a role in exerting top–down control on cognitive processing, they have been associated with different functional roles. Regions within the ECN are characterized by the flexibility of their representational content (Duncan, 2010) and ability to sustain distractor-resistant representations of information relevant for goal-directed processing (Waskom, Kumaran, Gordon, Rissman, & Wagner, 2014; Miller, Erickson, & Desimone, 1996). Dorsal attention regions, in contrast, appear to contain prioritized topographical maps of visual space (Silver & Kastner, 2009) that are used for internally directed visual attention (Corbetta & Shulman, 2002), a possible mechanism of visual WM maintenance (Sreenivasan, Curtis, & D'Esposito, 2014). Our results thus suggest that training reduces the demand on higher levels of a hierarchical system that supports the maintenance and updating of active WM traces.

WM training studies have reported multiple patterns of functional plasticity associated with gains in WM performance, including increased activations or decreased activations. The variety of changes in activation may reflect not only the variety of tasks but also the duration of training (ranging from a single session of training to our study of a month of intensive training) and the initial and final levels of performance. In our study, participants were considerably above chance in all conditions at the outset, improved their performance substantially in the more difficult conditions (which were far below their dual *n*-back capacity from the month of intensive training), and exhibited large reductions of activation in the more demanding conditions.

Training-related Changes in Functional Connectivity

WM training also increased frontoparietal functional connectivity during task performance, although these changes were observed only in the dual 2-back condition. In contrast to the changes in univariate activation, changes in within-network functional connectivity did not significantly differ between the ECN and DAN and between-network connectivity also increased. Furthermore, connectivity increases correlated with improvements in behavioral performance. It is unclear why connectivity (and activation) changes were modest in the 3-back condition given the robust behavioral improvements in that condition for the *n*-back group, though prior work suggests that encoding

strategies for difficult WM tasks can vary across participant's ability levels (Cusack, Lehmann, Veldsman, & Mitchell, 2009). This could have especially affected connectivity measurements at the pretraining dual 3-back level, when the task was quite challenging for many participants. The training-induced relations between brain plasticity as measured by connectivity and gains in WM performance are consistent with EEG studies examining the WM benefits of visual–perceptual (Mishra, Rolle, & Gazzaley, 2015; Berry et al., 2010) and distractor training (Mishra, de Villers-Sidani, Merzenich, & Gazzaley, 2014).

Conclusions

Interest in the dual *n*-back task arises from at least two sources. First, scientifically, the task is a complex WM task that exercises each of the putative constructs in the suite of "executive functions" (Miyake et al., 2000)—monitoring and maintenance in the encoding of incoming stimuli, inhibition in the avoidance of lure trials, and switching in the requirement of encoding stimuli from two domains simultaneously. Second, perhaps owing to the many WM processes engaged by this task, there has been some evidence that training on the dual *n*-back task transfers to other cognitive domains (Au et al., 2015; Kundu et al., 2013; Jaeggi et al., 2008). This transfer could have been the result of training-induced plasticity in a common neural substrate relevant to multiple cognitive domains (Dahlin, Neely, Larsson, Bäckman, & Nyberg, 2008; Jonides, 2004). Indeed, in this study there were large and specific functional changes in both activation and connectivity of the dorsolateral pFC and parietal brain regions known to be associated with human intelligence (Jung & Haier, 2007). Nevertheless, the robust training-induced plasticity did not support transfer to any other domain of cognition (Thompson et al., 2013).

Dual *n*-back training did, however, enable remarkable learning on the trained task itself, with some participants becoming able to perform a dual 9-back after 20 sessions of training. By the end of training, participants could perform the originally highly demanding 2-back and 3-back conditions with same ease (measured by speed and accuracy) as the minimally demanding 0-back and 1-back conditions. This was accompanied by large reductions of activation, specifically in the frontoparietal ECN, that were, by the end of training, no greater for the originally highly demanding 2-back and 3-back conditions than the minimally demanding 0-back and 1-back conditions. Furthermore, the task-specific growth of dual *n*-back WMC was associated with increased functional connectivity within and between the ECN and DAN. These findings, in the context of an active control training condition, reveal the anatomically specific nature of functional brain plasticity associated with the expansion of task-specific WMC. Although these particular gains did not enable far transfer to untrained measures, they do serve as a valuable exemplar of the plastic capacity of the human brain as it develops a remarkable mastery of a quite complicated and challenging task.

REFERENCES

Au, J., Sheehan, E., Tsai, N., Duncan, G. J., Buschkuehl, M., & Jaeggi, S. M. (2015). Improving fluid intelligence with training on working memory: A meta-analysis. *Psychonomic Bulletin & Review, 22,* 366–377.

Baddeley, A. (1992). Working memory. *Science, 255,* 556–559.

Berry, A. S., Zanto, T. P., Clapp, W. C., Hardy, J. L., Delahunt, P. B., Mahncke, H. W., et al. (2010). The influence of perceptual training on working memory in older adults. *PLoS One, 5,* 1–8.

Braver, T. S., Cohen, J. D., Nystrom, L. E., Jonides, J., Smith, E., & Noll, D. C. (1997). A parametric study of prefrontal cortex involvement in human working memory. *Neuroimage, 5,* 49–62.

Buschkuehl, M., Hernandez-Garcia, L., Jaeggi, S. M., Bernard, J. A., & Jonides, J. (2014). Neural effects of short-term training on working memory. *Cognitive, Affective & Behavioral Neuroscience, 14,* 147–160.

Cohen, J. D., Perlstein, W. M., Braver, T. S., Nystrom, L. E., Noll, D. C., Jonides, J., et al. (1997). Temporal dynamics of brain activation during a working memory task. *Nature, 386,* 604–608.

Corbetta, M., & Shulman, G. L. (2002). Control of goal-directed and stimulus-driven attention in the brain. *Nature Reviews Neuroscience, 3,* 201–215.

Curtis, C. E., & D'Esposito, M. (2003). Persistent activity in the prefrontal cortex during working memory. *Trends in Cognitive Sciences, 7,* 415–423.

Cusack, R., Lehmann, M., Veldsman, M., & Mitchell, D. J. (2009). Encoding strategy and not visual working memory capacity correlates with intelligence. *Psychonomic Bulletin & Review, 16,* 641–647.

Dahlin, E., Neely, A. S., Larsson, A., Bäckman, L., & Nyberg, L. (2008). Transfer of learning after updating training mediated by the striatum. *Science, 320,* 1510–1512.

Dale, A. M., Fischl, B., & Sereno, M. I. (1999). Cortical surface-based analysis. *Neuroimage, 9,* 179–194.

Daneman, M., & Carpenter, P. A. (1980). Individual differences in working memory and reading. *Journal of Verbal Learning and Verbal Behavior, 19,* 450–466.

Duncan, J. (2010). The multiple-demand (MD) system of the primate brain: Mental programs for intelligent behaviour. *Trends in Cognitive Sciences, 14,* 172–179.

Engle, R. W., Tuholski, S. W., Laughlin, J. E., & Conway, A. R. A. (1999). Working memory, short-term memory, and general fluid intelligence: A latent-variable approach. *Journal of Experimental Psychology. General, 128,* 309–331.

Finn, A. S., Kraft, M. A., West, M. R., Leonard, J. A., Bish, C. E., Martin, R. E., et al. (2014). Cognitive skills, student achievement tests, and schools. *Psychological Science, 25,* 736–744.

Gathercole, S. E., Pickering, S. J., Knight, C., & Stegmann, Z. (2004). Working memory skills and educational attainment: Evidence from national curriculum assessments at 7 and 14 years of age. *Applied Cognitive Psychology, 18,* 1–16.

Gorgolewski, K., Burns, C. D., Madison, C., Clark, D., Halchenko, Y. O., Waskom, M. L., et al. (2011). Nipype: A flexible, lightweight and extensible neuroimaging data processing framework in python. *Frontiers in Neuroinformatics, 5,* 13.

Greve, D. N., & Fischl, B. (2009). Accurate and robust brain image alignment using boundary-based registration. *Neuroimage, 48,* 63–72.

Hempel, A., Giesel, F. L., Garcia Caraballo, N. M., Amann, M., Meyer, H., Wüstenberg, T., et al. (2004). Plasticity of cortical activation related to working memory during training. *American Journal of Psychiatry, 161,* 745–747.

Jaeggi, S. M., Buschkuehl, M., Etienne, A., Ozdoba, C., Perrig, W. J., & Nirkko, A. C. (2007). On how high performers keep cool brains in situations of cognitive overload. *Cognitive, Affective & Behavioral Neuroscience, 7,* 75–89.

Jaeggi, S. M., Buschkuehl, M., Jonides, J., & Perrig, W. J. (2008). Improving fluid intelligence with training on working memory. *Proceedings of the National Academy of Sciences, U.S.A., 105,* 6829–6833.

Jenkinson, M., Beckmann, C. F., Behrens, T. E. J., Woolrich, M. W., & Smith, S. (2012). FSL. *Neuroimage, 62,* 782–790.

Jonides, J. (2004). How does practice makes perfect? *Nature Neuroscience, 7,* 10–11.

Jung, R. E., & Haier, R. J. (2007). The parieto-frontal integration theory (P-FIT) of intelligence: Converging neuroimaging evidence. *Behavioral and Brain Sciences, 30,* 135–154.

Kelly, A. M. C., & Garavan, H. (2005). Human functional neuroimaging of brain changes associated with practice. *Cerebral Cortex, 15,* 1089–1102.

Klingberg, T. (2010). Training and plasticity of working memory. *Trends in Cognitive Sciences, 14,* 317–324.

Kundu, B., Sutterer, D. W., Emrich, S. M., & Postle, B. R. (2013). Strengthened effective connectivity underlies transfer of working memory training to tests of short-term memory and attention. *Journal of Neuroscience, 33,* 8705–8715.

Landau, S. M., Garavan, H., Schumacher, E. H., & D'Esposito, M. (2007). Regional specificity and practice: Dynamic changes in object and spatial working memory. *Brain Research, 1180,* 78–89.

Landau, S. M., Schumacher, E. H., Garavan, H., Druzgal, T. J., & D'Esposito, M. (2004). A functional MRI study of the influence of practice on component processes of working memory. *Neuroimage, 22,* 211–221.

Langer, N., von Bastian, C. C., Wirz, H., Oberauer, K., & Jäncke, L. (2013). The effects of working memory training on functional brain network efficiency. *Cortex, 49,* 2424–2438.

McNab, F., & Klingberg, T. (2008). Prefrontal cortex and basal ganglia control access to working memory. *Nature Neuroscience, 11,* 103–107.

Miller, E. K., Erickson, C. A., & Desimone, R. (1996). Neural mechanisms of visual working memory in prefrontal cortex of the macaque. *Journal of Neuroscience, 16,* 5154–5167.

Mishra, J., de Villers-Sidani, E., Merzenich, M., & Gazzaley, A. (2014). Adaptive training diminishes distractibility in aging across species. *Neuron, 84,* 1091–1103.

Mishra, J., Rolle, C., & Gazzaley, A. (2015). Neural plasticity underlying visual perceptual learning in aging. *Brain Research, 1612,* 140–151.

Miyake, A., Friedman, N. P., Emerson, M. J., Witzki, A. H., Howerter, A., & Wager, T. D. (2000). The unity and diversity of executive functions and their contributions to complex "frontal lobe" tasks: A latent variable analysis. *Cognitive Psychology, 41,* 49–100.

Olesen, P. J., Westerberg, H., & Klingberg, T. (2004). Increased prefrontal and parietal activity after training of working memory. *Nature Neuroscience, 7,* 75–79.

Owen, A. M., McMillan, K. M., Laird, A. R., & Bullmore, E. (2005). N-back working memory paradigm: A meta-analysis of normative functional neuroimaging studies. *Human Brain Mapping, 25,* 46–59.

Pinheiro, J., Bates, D., DebRoy, S., Sarkar, D., & R Core Team. (2015). *nlme: Linear and nonlinear mixed effects models.* https://cran.r-project.org/web/packages/nlme/citation.html.

Power, J. D., Cohen, A. L., Nelson, S. M., Wig, G. S., Barnes, K. A., Church, J. A., et al. (2011). Functional network organization of the human brain. *Neuron, 72,* 665–678.

Pylyshyn, Z. W., & Storm, R. W. (1988). Tracking multiple independent targets: Evidence for a parallel tracking mechanism. *Spatial Vision, 3,* 179–197.

Raven, J. C., Court, J. H., & Raven, J. (1998). *Raven's progressive matrices.* Oxford: Oxford Psychological Press.

Redick, T. S., Shipstead, Z., Harrison, T. L., Hicks, K. L., Fried, D. E., Hambrick, D. Z., et al. (2013). No evidence of intelligence improvement after working memory training: A randomized, placebo-controlled study. *Journal of Experimental Psychology: General, 142,* 359–379.

Schneiders, J. A., Opitz, B., Krick, C. M., & Mecklinger, A. (2011). Separating intra-modal and across-modal training effects in visual working memory: An fMRI investigation. *Cerebral Cortex, 21,* 2555–2564.

Schneiders, J. A., Opitz, B., Tang, H., Deng, Y., Xie, C., Li, H., et al. (2012). The impact of auditory working memory training on the frontoparietal working memory network. *Frontiers in Human Neuroscience, 6,* 173.

Schweizer, S., Grahn, J., Hampshire, A., Mobbs, D., & Dalgleish, T. (2013). Training the emotional brain: Improving affective control through emotional working memory training. *Journal of Neuroscience, 33,* 5301–5311.

Silver, M. A., & Kastner, S. (2009). Topographic maps in human frontal and parietal cortex. *Trends in Cognitive Sciences, 13,* 488–495.

Smith, E., & Jonides, J. (1997). Working memory: A view from neuroimaging. *Cognitive Psychology, 33,* 5–42.

Smith, S., & Brady, J. (1997). SUSAN—A new approach to low level image processing. *International Journal of Computer Vision, 23,* 45–78.

Smith, S., Jenkinson, M., Woolrich, M. W., Beckmann, C. F., Behrens, T. E. J., Johansen-Berg, H., et al. (2004). Advances

in functional and structural MR image analysis and implementation as FSL. *Neuroimage, 23,* S208–S219.

Smith, S., Miller, K. L., Salimi-Khorshidi, G., Webster, M., Beckmann, C. F., Nichols, T. E., et al. (2011). Network modelling methods for fMRI. *Neuroimage, 54,* 875–891.

Sreenivasan, K. K., Curtis, C. E., & D'Esposito, M. (2014). Revisiting the role of persistent neural activity during working memory. *Trends in Cognitive Sciences, 18,* 82–89.

Thompson, T. W., Gabrieli, J. D. E., & Alvarez, G. A. (2010). Adaptive training in multiple object tracking expands attentional capacity. *Journal of Vision, 10,* 308.

Thompson, T. W., Waskom, M. L., Garel, K.-L. A., Cardenas-Iniguez, C., Reynolds, G. O., Winter, R., et al. (2013). Failure of working memory training to enhance cognition or intelligence. *PloS One, 8,* e63614.

Vincent, J. L., Kahn, I., Snyder, A. Z., Raichle, M. E., & Buckner, R. L. (2008). Evidence for a frontoparietal control system revealed by intrinsic functional connectivity. *Journal of Neurophysiology, 100,* 3328–3342.

Wager, T. D., & Smith, E. (2003). Neuroimaging studies of working memory: A meta-analysis. *Cognitive, Affective & Behavioral Neuroscience, 3,* 255–274.

Waskom, M. L., Kumaran, D., Gordon, A. M., Rissman, J., & Wagner, A. D. (2014). Frontoparietal representations of task context support the flexible control of goal-directed cognition. *Journal of Neuroscience, 34,* 10743–10755.

Wechsler, D. (1999). *Wechsler Abbreviated Scale of Intelligence.* New York: Psychological Corporation.

Woolrich, M. W., Ripley, B. D., Brady, M., & Smith, S. (2001). Temporal autocorrelation in univariate linear modeling of fMRI data. *Neuroimage, 14,* 1370–1386.

Yeo, B. T. T., Krienen, F. M., Sepulcre, J., Sabuncu, M. R., Lashkari, D., Hollinshead, M., et al. (2011). The organization of the human cerebral cortex estimated by intrinsic functional connectivity. *Journal of Neurophysiology, 106,* 1125–1165.

Yoo, S.-S., Paralkar, G., & Panych, L. P. (2004). Neural substrates associated with the concurrent performance of dual working memory tasks. *International Journal of Neuroscience, 114,* 613–631.